U–Pb, Pb–Pb and Sm–Nd ages of davidite within albitite zone from Bichun, Jaipur district, Rajasthan, India: possible link between uranium mineralization and Grenvillian orogeny

G. S. Yadav[1,*], U. K. Pandey[2], S. L. Aravind[3], P. K. Panchal[3], A. S. Venkatesh[4], P. R. Sahoo[4], A. K. Chaturvedi[2], A. K. Rai[2] and P. S. Parihar[2]

[1]Atomic Minerals Directorate for Exploration and Research, Jamshedpur 831 002, India
[2]Atomic Minerals Directorate for Exploration and Research, Hyderabad 500 016, India
[3]Atomic Minerals Directorate for Exploration and Research, Jaipur 302 030, India
[4]Department of Applied Geology, Indian Institute of Technology (Indian School of Mines), Dhanbad 826 004, India

Uranium mineralization in Bichun area, Jaipur district, Rajasthan, India is hosted by albitites within the Banded Gneissic Complex (BGC). Detailed mineralogical and EPMA studies reveal the presence of davidite along with brannerite and uraninite. The U–Pb concordia upper intercept age of 933 ± 13 Ma and Pb–Pb isochron age of 930 ± 4 Ma, on pure davidite fractions indicate the timing of uranium mineralizing event to be ca. 930 Ma. The timing of uranium mineralization can be correlated with the Grenvillian orogeny (ca. 1000 Ma). The Sm–Nd model age (T_{DM}) of davidites varies from 1851 to 2200 Ma with $\varepsilon_{Nd(930\ Ma)}$ ranging from –10.7 to –15.5 which shows that the Palaeoproterozoic rocks with crustal component (either within BGC or basement granite) are the source for uranium.

Keywords: Albitite zone, davidite, geochronology, orogeny, uranium mineralization.

DAVIDITE is a primary refractory uranium mineral that consists of U, REE, Fe and Ti. Uranium mineralization occurs spatially, temporally and genetically with albitites in Ukraine, Sweden, Brazil, Guyana and Australia[1]. Most of these deposits are Proterozoic and some are coincident with the assemblage of Rodinia/Grenvillian event. The Grenvillian (ca. 1.0 Ga) orogeny marks an important but not well understood period in the Earth's history, because it is not fully described in many continents[2–5]. Occurrence of Grenvillian orogenic belts in several parts of the world has been reported based on U–Pb age data on zircons, albeit their reported conspicuous near absence from Asia[4]. The assemblage of Rhodinian/Grenvillian orogeny is reported from the Eastern Ghats Belt which was correlated with East Antarctica, though the geological set-up, metal association and ages clearly are synonymous with such an important global event[5]. In Rajasthan, India, within the Banded Gneissic Complex (BGC) of Aravalli–Delhi Fold Belt (ADFB), Neoproterozoic ages (0.97–0.93 Ga) are related to Grenvillian orogeny, wherein different dispersed blocks amalgamated together to form the Rhodinia supercontinent[1,6]. The global Grenvillian orogeny has been documented in the crustal domains and constrains the timing of the metamorphic event in the BGC of central Rajasthan[7].

The study area, Bichun (lat. 26°47′36″–26°49′41″, long. 75°20′41″–75°20′43″), Jaipur district, Rajasthan, is part of the BGC, and lies 50 km SW of Jaipur (Figure 1) in western India. Uranium mineralization associated with davidite in Bichun area is hosted by albitite within the BGC. Significant uranium mineralization (up to 6.4% U_3O_8) with REE, Y and Sc has been reported in association with albitized rocks of the BGC terrain near Bichun, where davidite occurs as one of the major ore minerals[8]. The established uranium mineralization of Rajasthan is well recorded within the North Delhi Fold Belt (NDFB) around Rohil, Sikar district, which is shear-controlled, vein-type and hosted by albitized metasediments of Ajabgarh Group of Delhi Supergroup along the eastern part of the Khetri sub-basin. The 320 km long albitite zone extending from Dhancholi in the NE (Mahendragarh district, Haryana) to Tal in the SW (Rajsamand district, Rajasthan) is the main host of uranium mineralization in NDFB[9–12].

Multi-method geochronological studies have been conducted on pure separated davidite grains from albitites in the BGC using multi-collector Thermal Ionisation Mass Spectrometer (TIMS)-Isotopex. Various workers dated davidite mineral previously using TIMS as well as Laser Ablation High Resolution Inductively Coupled Plasma Mass Spectrometer (LA-HR-ICPMS)[13–16]; both the techniques gave similar results. Attempts have also been made to date davidite using TIMS with an aim to constrain the age of uranium mineralization, source for uranium and correlation of time of uranium mineralization with the geological events in the present study area. Finally, this study will assist in understanding the metallogeny in this part of NDFB and its correlation with the Grenvillian event, which could be of help in uranium exploration in areas having similar age and geological setting.

The area around Bichun is part of the BGC[17,18] and the main rock types are migmatite, granite gneiss, amphibolite, quartzite and mica schist intruded by quartzofeldspathic and albitite injections. BGC is a polymetamorphic terrain[17], which preserves records of crustal evolution for a period of >2.0 Ga spanning ~3.3 to ~1.0 Ga. It is further divided into two tectonic domains on the basis of contrasting geochronology, which in the southern part (BGC-I) exclusively preserves the Archaean age. On the contrary, the northern part (BGC-II) dominantly has Palaeo-Neoproterozoic age[7]. The study area

*For correspondence. (e-mail: gsyadav.amd@gov.in)

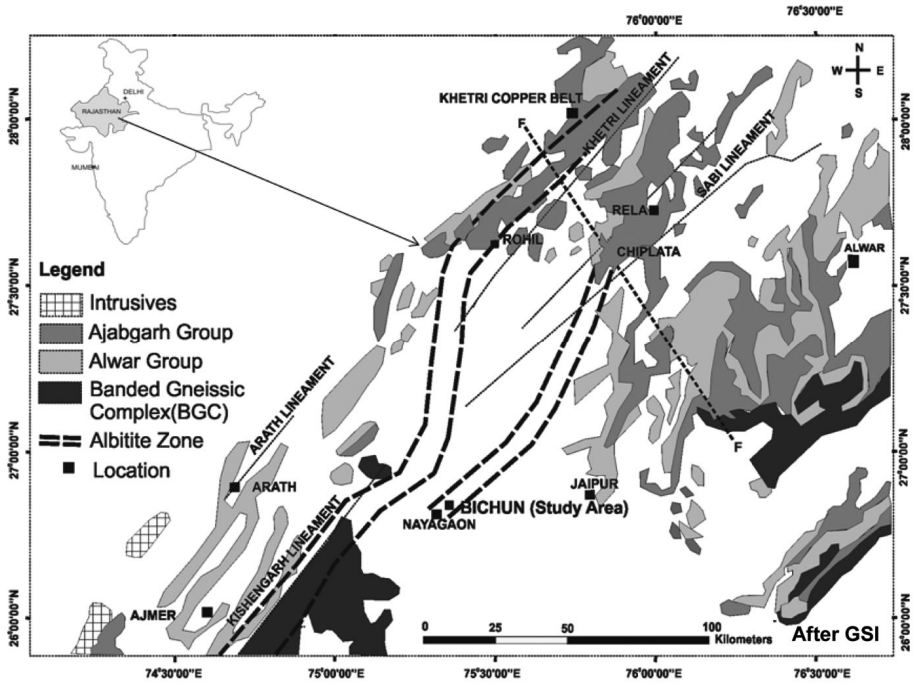

Figure 1. Geological map showing the albitite zones in Rajasthan, India and location of davidite in and around Bichun area (study area), Jaipur district, Rajasthan.

falls in the northern part, i.e. within BGC-II. The general trend of the litho-units varies from N–S to NNE–SSW to NNW–SSE (Figure 1). The area is deformed by intense folding and faulting events, which is reflected on the complex structural fabric of the area. The albitite body is conformable to the general trend of the foliations of the country rock (NNE–SSW). The albitites are light pink, fine- to medium-grained with saccharoidal texture and, in places, are coarse-grained from a few millimetres to 7–8 cm (refs 18 and 19). The area under study forms a southwestern trending zone of albitization which commences in the BGC and transgresses into the NDFB meta-sediments towards northeast. These occurrences form a linear zone extending over a length of about 130 km, with 5–12 km width from Bichun–Nayagaon in the south to Rela–Gasipura in the north. This zone has a regional NE–SW trend and occurs about 20–40 km east of the known albitite line[8,9]. The albitite bodies in Bichun area are lensoidal and intrude the BGC. The enclaves of country rock, i.e. BGC in albitite indicate the intrusive nature of albitite. Davidite occurs as fracture fillings, veins and disseminations within albitite, which suggest, its introduction by hydrothermal activity (Figure 2 *a* and *b*). The albitites exhibit deep fracture control for their emplacement[7].

Davidite, a primary REE-bearing radioactive mineral occurs in a wide range of environments. It has been observed that davidite occurs spatially, temporally and genetically within Proterozoic albitites and its association with Grenvillian event is noticeable in several places[1]. In the field, davidite is found to be associated with fine- to medium-grained albitized rocks (Figure 2 *a*). Field observations, petrographic and EPMA studies indicate davidite as a major ore mineral along with brannerite, uraninite, ilmenite, magnetite and leucoxene. The gangue minerals include quartz, albite, chlorite, sphene, rutile and epidote. Fresh davidite grains exhibit sub-metallic lustre and broken surfaces exhibit conchoidal fractures. Under reflected light, davidite is grey with brownish tint, exhibiting about 15% reflectance (Figure 2 *c* and *d*). In majority of cases, davidite grains are associated with sphene (Figure 2 *c* and *d*). Intergrowth of irregular ilmenite patches within davidite is a common feature in the study area (Figure 2 *c*). Radioactivity from davidite within sphene occurs as thick haloes, detected after a careful variable-density alpha track-petrography on several radioactive samples from the study area (Figure 2 *d*).

Davidite samples have been chosen carefully across the entire albitite zone after high-resolution sampling. Further, these samples have been petrographically characterized and confirmed by XRD studies as well. About 99% pure davidite was obtained for the geochronological studies after a careful heavy media separation (using bromoform and methylene iodide) and hand-picking under binocular microscope. Eight pure fractions of davidite mineral samples were dissolved using conc. HF, HNO_3 and 8 M HCl. Separate aliquots for spike and unspike analyses were taken from the solutions. Elemental separation of Sm, Nd, U and Pb from the solutions was carried out in class-100 clean chemical laboratory by ion

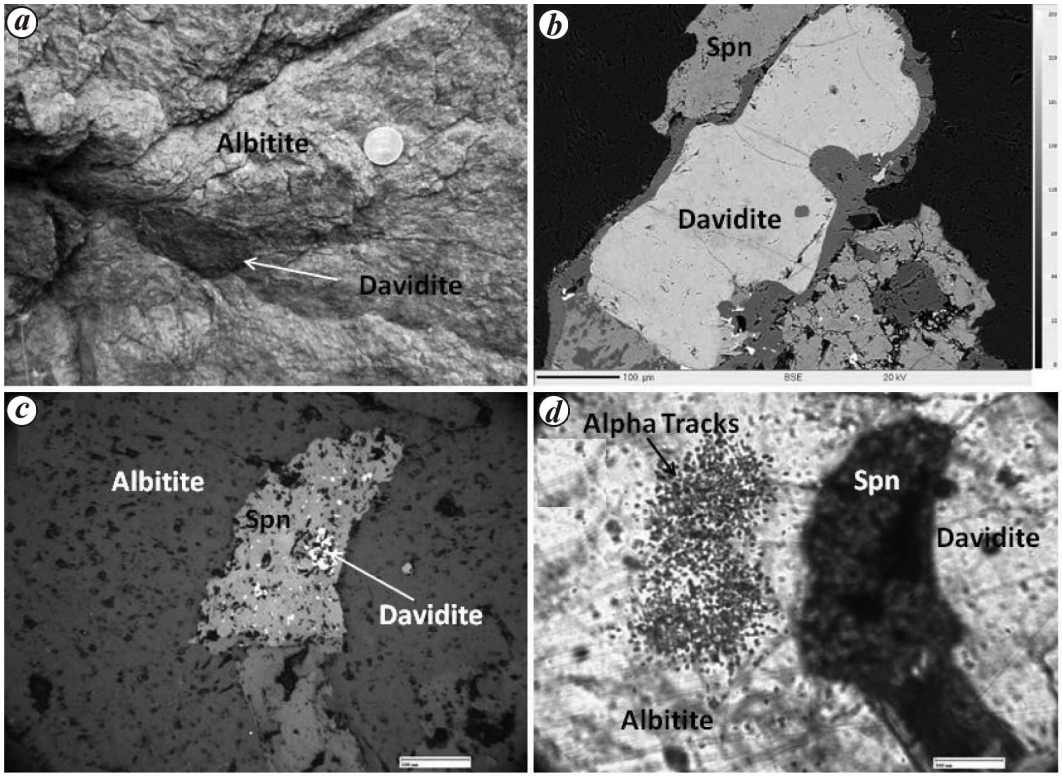

Figure 2. Nature of davidite occurrence within albitized rocks along with associated radioactive phases. ***a***, Field relationships showing davidite in the form of lumps and elongated veinlets within the albitite rock. ***b***, EPMA–BSE image of a large davidite crystal with minute inclusions of ilmenite and silicates, surrounded by sphene. ***c***, Photomicrograph of a sphene grain with inclusions of davidite (bright spots). ***d***, Radioactivity within sphene (Spn) grain as exhibited by low to moderate density alpha tracks in albitite, Bichum area, Jaipur district.

exchange and separated pure salts of these elements were analysed for their isotopic ratios using multi-collector TIMS-Phoenix-Isotopx instrument. Isotopic abundances were obtained using isotope dilution mass spectrometry (IDMS). The in-run isotope fractionation correction for $^{143}Nd/^{144}Nd$ ratio was applied using $^{146}Nd/^{144}Nd$ ratio of 0.7219. The 2σ analytical error in $^{206}Pb/^{204}Pb$, $^{207}Pb/^{204}Pb$ and $^{208}Pb/^{204}Pb$ ratios is 0.2%, whereas in Sm, Nd, U and Pb abundance estimation errors are 1%, based on the number of duplicate analyses. The radiogenic Pb standard (SRM983, $n = 8$) analysed gave $^{206}Pb/^{204}Pb$, $^{207}Pb/^{204}Pb$, $^{208}Pb/^{204}Pb$ ratios as 2707.3 ± 0.15%, 192.65 ± 0.17% and 36.828 ± 0.19% respectively, whereas $^{143}Nd/^{144}Nd$ and $^{145}Nd/^{144}Nd$ ratios obtained on JM Nd standard (NDN-1, $n = 7$) are 0.5111106 ± 0.001% and 0.348409 ± 0.0009% respectively. Isochron and concordia plots of Wetherill done using ISOPLOT v. 3 of Ludwig[20].

In total eight davidite fractions (GC4139A to GC4139D and GC4140A to GC4140D), from two davidite mineral samples, were analysed for U–Pb, Pb–Pb and Sm–Nd isotope systematics and the results are given in Table 1. In U–Pb systematics, U, Pb abundances, $^{206}Pb^*/^{238}U$ (*radiogenic) and $^{207}Pb^*/^{235}U$ ratios in the above davidite samples vary from 4.79% to 6.75%, 0.7% to 1.0%, 0.1515% to 0.1541% and 1.479% to 1.499% respectively. $^{238}U/^{204}Pb$ (T_6), $^{235}U/^{204}Pb$ (T_7) and $^{207}Pb^*/^{206}Pb^*$ ($T_{7/6}$) ages obtained on all the eight davidite fractions show minor discordance as the ages have narrow range, i.e. 909–924 Ma (T_6), 922–933 Ma (T_7) and 945–979 Ma ($T_{7/6}$) respectively, and show normal age trend, i.e. $T_6 < T_7 < T_{7/6}$ (Table 1). The U–Pb concordia plot for all these samples defined an age of 933 ± 13 Ma with MSWD (mean square weighted deviate) of 1.08 (Table 1 and Figure 3 *a*). In Pb–Pb systematics, the $^{206}Pb/^{204}Pb$, $^{207}Pb/^{204}Pb$ and $^{208}Pb/^{204}Pb$ ratios in these samples vary from 1496.6 to 7355.0, 121.27 to 532.91 and 72.993 to 172.91 respectively. All the eight davidite samples defined Pb–Pb isochron age of 930 ± 4 Ma with MSWD = 0.73 and $\mu_1 = 12.1 \pm 0.6$ (Table 1 and Figure 3 *b*).

In Sm–Nd systematics, Sm and Nd abundances in seven davidite fractions range from 265 to 330 ppm and 1911 to 2859 ppm respectively. The $^{147}Sm/^{144}Nd$ ratios in these davidites vary from 0.0640 to 0.1004, whereas $^{143}Nd/^{144}Nd$ varies from 0.511198 to 0.511398 (Table 1). The Sm–Nd data on these samples show large scatter on isochron plot and do not define isochron age. The $\varepsilon_{Ndi(930\ Ma)}$ estimated on these davidites varies from –10.7 to –15.5. The Sm–Nd model ages on these davidites (T_{DM}) vary from 1851 to 2200 Ma.

In Bichun area, the uraniferous zones run in a strike length of 1.7 km and width of 5–30 m with up to 6.4% U_3O_8 and negligible thorium[19]. The mineralization is

Table 1. U–Pb, Pb–Pb and Sm–Nd isotopic data on davidite samples across Bichun, Jaipur district, Rajasthan, India

Lab. ref. no.	Sample ID	U (%)	Pb (%)	Sm (ppm)	Nd (ppm)	$^{207}Pb^*/^{235}U$	$^{206}Pb^*/^{238}U$	$^{207}Pb^*/^{206}Pb^*$	$^{147}Sm/^{144}Nd$	$^{143}Nd/^{144}Nd$	$^{206}Pb/^{204}Pb$	$^{207}Pb/^{204}Pb$	$^{208}Pb/^{204}Pb$	T_6 (Ma)	T_7 (Ma)	$T_{7/6}$ (Ma)	Sm–Nd (T_{DM}; Ma)	ε_{Ndi} (930 Ma)
GC4139A	BCH/M/1	5.55	0.81	315	1911	1.492	0.1537	0.0707	0.1004	0.511398	7287.2	527.17	164.28	922	927	949 ± 0.1	2200	–12.7
GC4139B	BCH/M/1	5.58	0.81	330	2415	1.488	0.1536	0.0706	0.0832	0.511397	7251.3	523.69	164.12	921	926	945 ± 0.2	1910	–10.7
GC4139C	BCH/M/1	5.55	0.81	297	2044	1.499	0.1541	0.0709	0.0886	0.511346	7355.0	532.97	172.91	924	930	953 ± 0.1	2055	–12.4
GC4139D	BCH/M/1	5.36	0.77	–	–	1.479	0.1525	0.0707	–	–	6488.7	470.53	159.98	915	922	947 ± 0.1	–	–
GC4140A	BCH/V/1	6.75	1.00	265	2429	1.487	0.1515	0.0715	0.0665	0.511198	1938.6	152.29	83.040	909	925	972 ± 0.3	1899	–12.6
GC4140B	BCH/V/1	4.92	0.73	305	2859	1.491	0.1518	0.0716	0.0650	0.511044	1822.2	144.08	80.325	911	927	974 ± 0.6	2037	–15. 5
GC4140C	BCH/V/1	4.98	0.75	291	2695	1.506	0.1529	0.0718	0.0657	0.511213	1496.6	121.27	72.993	917	933	979 ± 2.8	1873	–12.3
GC4140D	BCH/V/1	4.79	0.71	267	2543	1.493	0.1517	0.0717	0.0640	0.511214	1710.8	136.32	78.876	911	927	977 ± 0.3	1851	–12.0
% errors (2 σ)		2	1	1	1	0.5	0.5	0.2	1	0.005	0.2	0.2	0.2					

U–Pb concordia age 933 ± 13 Ma (MSWD = 1.08), Pb – Pb isochron age 930 ± 4 Ma (MSWD = 0.73), Sm–Nd (T_{DM}) age = 1851–2200 Ma, *Radiogenic.

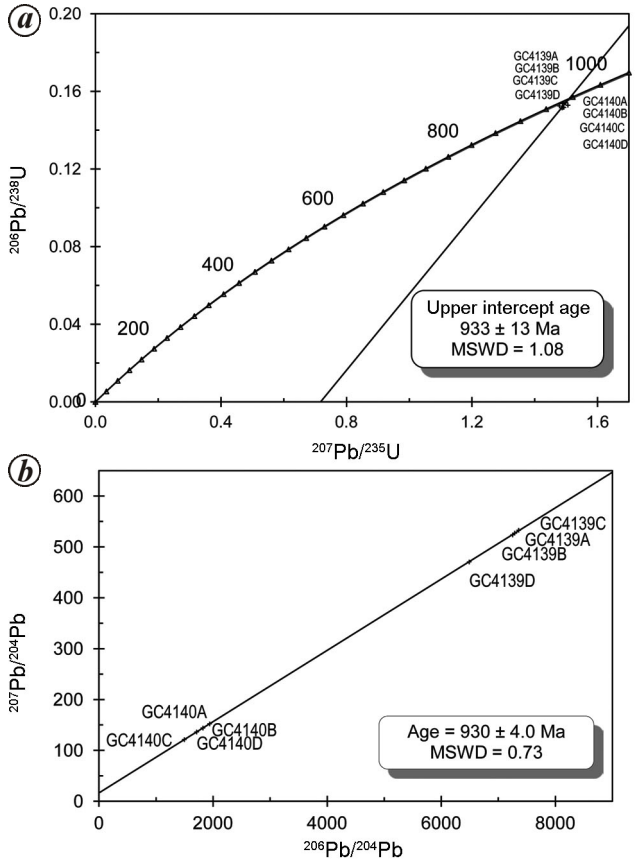

Figure 3. ***a***, U–Pb Concordia plot for davidite from Bichun. ***b***, Pb–Pb isochron age on davidite from Bichun.

hosted by albitites within the BGC characterized by migmatites and gneisses and having a different geological set-up than the already established uranium deposit in the NDFB which is associated with albitites in Delhi Supergroup of rocks of comparatively of lower metamorphic grade, in and around Rohil, Sikar district, Rajasthan[11,12]. Though ages of uranium mineralization from other parts of India have been reported earlier by the Atomic Minerals Directorate for Exploration and Research (AMD)[21–23], the ages of uranium mineralization in Bichun area are not known till date and are reported here. The prominent uranium mineral in Bichun is davidite with minor associated uranium minerals like brannerite and uraninite. Davidite occurs as disseminations and veins in albitites (Figure 2 *a*). Davidite and uraninite have been dated earlier both by TIMS and HR-LA-ICPMS, from uranium deposits of northern Australia, and ages obtained by both the instruments were similar[16].

The results of multi-method geochronological study (U–Pb, Pb–Pb and Sm–Nd) using TIMS, on eight pure davidite mineral fractions, separated from host albitites from Bichun, are reported here. The U–Pb concordia plot for all these samples defined an age of 933 ± 13 Ma with MSWD of 1.08 (Table 1 and Figure 3 *a*). Whereas the same set of samples yielded Pb–Pb isochron age of 930 ± 4 Ma with MSWD = 0.73 and model $\mu_1 = 12.1 \pm 0.6$ (Table 1 and Figure 3 *b*). It is clear from both U–Pb concordia upper intercept age as well as Pb–Pb isochron age on davidite that uranium mineralization in albitites from the BGC in Bichun has taken place at ca. 930 Ma. This age matches well with that of Neoproterozoic metamorphic event (940–950 Ma) within polymetamorphic BGC II (central Aravalli BGC) as reported, based on zircon U–Pb ages from migmatized ortho gneisses and magmatic charnockites[24,25]. The Neoproterozoic metamorphism at 1000 Ma has been reported from the Delhi Fold Belt (968 Ma, radiogenic Pb zircon age[25]; 945–952 Ma, Monazite EPMA age (C. Reeves, unpublished); 978 Ma, garnet Pb–Pb (Pb SL) isochron age[26], 987–986 Ma, U–Pb zircon and Pb isotopic data on galena from SW portion of the Delhi-Aravalli belt)[27]. The precise dates obtained from the present study indicate the effect of Grenvillian orogeny in the BGC as well as in the Delhi Fold Belt of Rajasthan. The earlier workers also reported Grenvillian orogeny from Rajasthan and other parts of India[7,23].

In a similar study, U–Pb, Rb-Sr and Sm–Nd systematics have been used to obtain the age of uranium mineralization elsewhere[28,29]. Majority of the Pb–Pb ages of brannerite and uraninite from albitite-hosted Valhalla uranium deposit, Queensland, Australia, are between 800 and 1150 Ma, which broadly corresponds to Grenville orogeny[1] and analogous correlations are shown elsewhere at about 0.7–1.0 Ga (refs 3, 5). The episode of uranium mineralization at Bichun during ca. 930 Ma may correspond to Grenvillian orogeny in the BGC in the process of evolution of various sub-basins and imposing metallotectonics suitable for radioactive and other mineralizations. The Sm–Nd model ages (T_{DM}) on davidites vary from 1851 to 2200 Ma. However, $\varepsilon_{Ndi\ (930\ Ma)}$ estimated on these davidite samples yields values range from –10.7 to –15.5. The negative $\varepsilon_{Ndi\ (930\ Ma)}$ and T_{DM} ages (1851–2200 Ma) of davidite indicate that the crustal rocks of Palaeoproterozoic age are the probable source for uranium in davidite of the Bichun area. U–Pb zircon data for BGC from central Aravalli yields Palaeoproterozoic age, which was earlier considered as Archean[22] and the davidite mineralization is an integral part of BGC in Bichun. Therefore, the BGC at Bichun which hosts albitite-related uranium mineralization might also be of the same age and is the probable source of uranium in davidites as inferred from the Sm–Nd T_{DM} ages (1851–2200 Ma). The high-grade rocks of BGC not only acted as the source for U, but also for Ti and Fe generally found abundant in such rocks to form davidite. These metals may be a part of metamorphic fluid generated during high grade of metamorphism and anatexis during Grenvillian orogeny. There is another possibility that the Palaeoproterozoic granites underlying the Delhi Supergroup of rocks[30,31] may have acted as a source for uranium during Grenvillian orogeny and Ti, Fe from the BGC joined together to form davidite. The

albitites might have genetic link with the above granites as reported earlier in the Khetri basin[28,31] and acted as hosts for uranium mineralization in favourable structural locales.

Thus, the new U–Pb concordia upper intercept age of 933 ± 13 Ma (MSWD of 1.08) and Pb–Pb isochron age of 930 ± 4 Ma (MSWD = 0.730), for davidite from Bichun area indicate timing of uranium mineralization hosted by the albitite rocks within the BGC.

The age of uranium mineralization may be correlated with Grenvillian orogeny (ca. 1000 Ma). Evidence of this major tectono–magmatic–thermal activity is present not only in BGC but also in the Aravalli and Delhi Supergroup of rocks in the form of upper amphibolite grade of metamorphism and magmatism.

Sm–Nd model ages (T_{DM}) of 1851–2200 Ma and negative $\varepsilon_{Ndi\,(930Ma)}$ of −10.7 to −15.5 obtained on davidites show that the crustal rocks of Palaeoproterozoic age are a source of uranium in davidite. The source rocks may be either the BGC itself or associated granites.

The concordia upper intercept U–Pb and Pb–Pb isochron ages of albitite-hosted davidite from the Bichun area, i.e. ca. 930 Ma, may help in modelling for uranium exploration related to albitite-hosted uranium mineralization elsewhere in a similar set-up.

1. Polito, P. A., Kyser, T. K. and Stanley, C., The Proterozoic, albitite-hosted, Valhalla uranium deposit, Queensland, Australia: a description of the alteration assemblage associated with uranium mineralisation in diamond drill hole V39. *Miner. Deposita*, 2009, **44**, 11–40.
2. Lentz, D., Mo, U. and REE mineralization in late-tectonic granitic pegmatites, south west Grenville Province, Canada. *Ore Geol. Rev.*, 1996, **11**, 97–227.
3. Tack, L., Wingate, M. T. D., Liegeois, J. P., Fernandez-Alonso, M. and Deblond, A., Early Neoproterozoic magmatism (1000–910 Ma) of the Zadinian and Mayumbiam Groups (Bas Congo): onset of Rodinia rifting at the western edge of the Congo Craton. *Precambrian Res.*, 2001, **110**, 277–306.
4. Rino, S., Kon, Y., Sato, W., Maruyam, S., Santosh, M. and Zhao, D., The Grenvillian and Pan-African orogens: world's largest orogenies through geologic time, and their implications on the origin of superplume. *Gondwana Res.*, 2008, **14**, 51–72.
5. Santosh, M., Maruyama, S. and Yamamoto, S., The making and breaking of supercontinents: some speculations based on superplumes, super downwelling and the role of tectosphere. *Gondwana Res.*, 2009, **15**, 324–341.
6. Yadav, G. S., Muthamilselvan, A., Shaji, T. S., Nanda, L. K. and Rai, A. K., Recognition of a new albitite zone in northern Rajasthan: its implications on uranium mineralization. *Curr. Sci.*, 2015, **108**(11), 1994–1998.
7. Ray, S. K., The albitite line of northern Rajasthan – a fossil intracontinental rift zone. *J. Geol. Soc. India*, 1990, **36**, 413–423.
8. Singh, G., Singh, R., Sharma, D. K., Yadav, O. P. and Jain, R. B., Uranium and REE potential of the albitite–pyroxenite–microclinite belt of Rajasthan, India. *Explor. Res. At. Miner.*, 1998, **11**, 1–12.
9. Yadav, O. P., Hamilton, S., Vimal, R., Saxena, S. K., Pande, A. K. and Gupta, K. R., Metasomatite–albitite-hosted uranium mineralization in Rajasthan. *Explor. Res. At. Miner.*, 2002, **14**, 109–130.
10. Khandelwal, M. K. *et al.*, Uranium–copper–molybdenum association in the Rohil deposit, North Delhi Fold Belt, Rajasthan. *Mem. Geol. Soc. India*, 2008, **73**, 117–130.
11. Bjorlykke, A., Cumming, G. L. and Krstic, D., New isotopic data from davidites and sulfides in the Bidjovagge gold–copper deposit, Finnmark, northern Norway. *Mineral. Petrol.*, 1990, **43**, 1–21.
12. Fryer, B. J., Jackson, S. E. and Longrich, H. P., The application of laser ablation microprobe-inductively coupled plasma-mass spectrometry (LAM–ICPMS) to *in situ* (U)–Pb geochronology. *Chem. Geol.*, 1993, **109**, 1–8.
13. Fayek, M., Harrison, T. M., Grove, M. and Coath, C. D., A rapid *in situ* method for determining the ages of uranium oxide minerals. *Int. Geol. Rev.*, 2000, **42**, 163–171.
14. Chipley, D., Polito, P. A. and Kyser, T. K., Measurement of U–Pb ages of uraninite and davidite by laser ablation-HR-ICP-MS. *Am. Mineral.*, 2007, **92**, 1925–1935.
15. Heron, A. M., The geology of central Rajasthan. *Mem. Geol. Surv. India*, 1953, **79**, 389.
16. Shaji, T. S., Nautiyal, K., Yadav, G. S., Yadav, O. P., Nanda, L. K. and Maithani, P. B., Occurrence of metamictdavidite, brannerite, and uraninite bearing albitite and albitised gneisses and the Banded Gneissic Complex around Bichun and Nayagaon areas, Jaipur district, Rajasthan India. *Explor. Res. At. Miner.*, 2011, **21**, 21–26.
17. Olerud, S., Davidite–loveringite in early Proterozoic albite felsite in Finnmark, north Norway. *Mineral. Mag.*, 1988, **52**, 400–402.
18. Ludwig, K. R., ISOPLOT – a geochronological toolkit for Microsoft Excel, Berkeley Geochronology Center, Special Publication, USA, 1993, No. 4, pp. 1–70.
19. Buick, I. S., Allen, C., Pandit, M., Rubatto, D. and Hermann, J., The Proterozoic magmatic and metamorphic history of the Banded Gneiss Complex, central Rajasthan, India: LA-ICP-MS U–Pb zircon constraints. *Precambrian Res.*, 2006, **151**, 119–142.
20. Pandit, M. K., Carter, L. M., Ashwal, L. D., Tucker, R. D., Torsvik, T. H., Jamtveit, B. and Bhushan, S. K., Age, petrogenesis and significance of 1 Ga granitoids and related rocks from the Sendra area, Aravalli craton, NW India. *J. Asian Earth Sci.*, 2003, **22**, 363–381.
21. Pant, N. C., Kundu, A. and Joshi, S., Age of metamorphism of Delhi Supergroup of rocks – electron microprobe ages from Mahendragarh district, Haryana. *J. Geol. Soc. India*, 2008, **72**, 365–372.
22. Pandey, U. K., Pandey, B. K., Krishna, K. V. G., Nanda, L. K. and Maithani, P. B., Rb–Sr and Pb–Pb age data from Delhi and Aravalli Supergroups of Rajasthan, India: temporal evidence for Neoproterozoic Gondwana geodynamics. In Abstract volume, 8th International Symposium on Gondwana to Asia 'Supercontinent Dynamics: India and Gondwana', NGRI, Hyderabad, 26–28 August 2011, pp. 70–71.
23. Deb, M., Thorpe, R. I., Krstic, D., Corfu, F. and Davis, D. W., Zircon U–Pb and galena Pb isotope evidence for an approximate 1.0 Ga terrane constituting the western margin of the Aravalli–Delhi orogenic belt, northwestern India. *Precambrian Res.*, 2001, **108**, 195–213.
24. Turpin, L., Maruejo, P. and Cuney, M., Chronology of granitic basement, hydrothermal albitites and uranium mineralization (Lagoa Real, South-Bahia, Brazil). *Contrib. Mineral. Petrol.*, 1988, **98**, 139–147.
25. Kaur, P., Chaudhry, N., Hofmann, A. W., Raczek, I., Okrusch, M., Skora, S. and Koepke, J., Metasomatism of ferroan granites in the northern Aravalli orogen, NW India: geochemical and isotopic constraints, and its metallogenic significance. *Int. J. Earth Sci.*, 2014, **103**, 1083–1112.
26. Kaur, P., Zehb, A., Chaudhri, N., Gerdes, A. and Okrusch, M., Archaean to Palaeoproterozoic crustal evolution of the Aravalli

mountain range, NW India, and its hinterland: the U–Pb and Hf isotope record of detrital zircon. *Precambrian Res*., 2011, **187**, 155–164.
27. Dwivedi, A. K., Pandey, U. K., Murugan, C., Bhatt, A. K., Ramesh Babu, P. V. and Joshi, M., Geochemistry and geochronology of A-type Barabazar granite – implications on the geodynamics of the South Purulia Shear Zone, *Singhbhum craton*, Eastern India. *J. Geol. Soc. India*, 2011, **77**, 527–838.
28. Pandey, B. K., Krishna, V., Pandey, U. K. and Sastry, D. V. L. N., Radiometric dating of uranium mineralisation in the Proterozoic basins of eastern Dharwar craton, South India. In Proceedings of the International Conference on Peaceful Uses of Atomic Energy, New Delhi, 2009, vol. 1, pp. 116–117.
29. Rai, A. K., Pandey, U. K., Zakaulla, S. and Parihar, P. S., New Pb–Pb (PbSL) age of dolomites from Vempalle Formation, Lower Cuddapah Supergroup, Kadapa, India: implication on age of uranium mineralization. *J. Geol. Soc. India*, 2015, **86**, 131–136.
30. Bhowmik, S. K., Bernhardt, H.-J. and Dasgupta, S., Grenvillian age high-pressure upper amphibolite–granulite metamorphism in the Aravalli–Delhi Mobile Belt, northwestern India: new evidence from monazite chemical age and its implication. *Precambrian Res*., 2010, **178**, 168–184.
31. Meert, J. G. *et al.*, Precambrian crustal evolution of Peninsular India: a 3.0 billion year odyssey. *J. Asian Earth Sci.*, 2010, **39**, 482–515.

ACKNOWLEDGEMENTS. We thank the Geochronology Laboratory, AMD, Hyderabad, for analytical support and the Indian School of Mines, Dhanbad for EPMA analyses. We also thank Prof. N. V. Chalapathi Rao and two anonymous reviewers for their suggestions, which helped improve the manuscript.

Received 20 December 2015; revised accepted 3 April 2016

doi: 10.18520/cs/v111/i5/907-913

Constraints on source parameters of the 25 April 2015, M_w = 7.8 Gorkha, Nepal earthquake from synthetic aperture radar interferometry

K. M. Sreejith[1,*], P. S. Sunil[2], Ritesh Agrawal[1], D. S. Ramesh[2] and A. S. Rajawat[1]

[1]Geosciences Division, Space Applications Centre (ISRO), Ahmedabad 380 015, India
[2]Indian Institute of Geomagnetism (DST), Navi Mumbai 410 218, India

We present InSAR observations of the co-seismic deformation caused by the M_w 7.8 Gorkha, Nepal earthquake. Analysis of Sentinel-1 data revealed about 100 × 100 sq. km surface deformation with ~1 m upliftment near Kathmandu, and ~0.8 m subsidence towards north along the line of sight of the satellite. The maximum deformation is observed about 40 km east–southeast of the epicentre, suggesting eastward propagation of the rupture. Elastic dislocation modelling revealed that the overall rupture occurred on a 170 km long, 60 km wide fault along the strike (286°) and dipping north (dip = 15°) with large amount of slip (4.5 m) confined to the centre (95 × 22 sq. km) and less slip (0.25 m) on the surrounding part of the fault plane. The corresponding moment magnitude is M_w 7.75. The area, depth and dip of the modelled fault plane are fairly consistent and overlap with the location of mid-crustal ramp in the Main Himalayan Thrust. We infer that the earthquake was possibly caused by the release of inter-seismic strain energy accumulated in the environs of mid-crustal ramp due to plate boundary forces.

Keywords: Co-seismic deformation, Gorkha, Nepal earthquake, synthetic aperture radar interferometry, source model.

THE catastrophic 25 April 2015 Gorkha, Nepal earthquake of magnitude M_w 7.8 located between Pokhara and Kathmandu (28.147°N and 84.708°E)[1,2] is one of the largest earthquakes to have struck Nepal since the 1934 Nepal-Bihar earthquake of M_w 8.2 (ref. 3). The earthquake caused widespread destruction in Nepal and parts of India and China with the total death toll exceeding 9000 and also injuring 23,000 in an area inhabited by about 8 million people. Moment tensor solutions from telesiesmic data suggest that the Nepal earthquake occurred on a 10–20° dipping sub-horizontal blind thrust fault at about 15 km depth with a strike of 290° from the north[1]. The M_w 7.8 event was followed by 553 aftershocks with magnitude >4, including two events having magnitudes 6.1 and 6.6 on the same day[4,5]. The largest aftershock occurred on 12 May 2015, about 150 km east of the main shock (Figure 1).

Of the several large, devastating historical earthquakes that occurred in the Himalayan region, only four were instrumentally recorded: the 1897 Shillong Plateau, 1905 Kangra, 1934 Nepal–Bihar and the 1950 Assam earthquakes (Figure 1). These are the largest known earthquakes to have occurred at the intersection of basement and the décollement thrust faults that ruptured ~1400 km of the Himalayan detachment[6]. However, geodetic data of these earthquakes were either incomplete or not available[7], and hence the epicentral location and source parameters of these earthquakes remain elusive. Therefore, precise measurement of the surface deformation caused by the 2015 Nepal earthquake has special importance from the perspective of tectonics of large earthquakes in the Himalaya. Earlier, the 1999 Chamoli (M_w = 6.6) and 2005 Kashmir (M_w = 7.6) earthquakes in the NW Himalayan region were studied using space geodetic techniques to

*For correspondence. (e-mail: sreejith81@gmail.com)